MT occurs through nucleation and growth. Upon cooling, martensite starts to develop from a temperature M_s and the growth finishes at M_f. Similarly, while heating, A_s and A_f denote austenite start and finish temperatures respectively. In order to understand the irreversible region of first order transition, we have performed a careful resistivity investigation across the MT. The region of irreversibility begins at A_f = 231 K and it closes at M_f = 198 K. Minor hysteresis loops (MHL) have been recorded between temperatures A_f and M_f by reversing the direction of heating/cooling. The resistivity data traces a different path as compared to full heating-cooling envelope curve (fig. A.5.2). The existence of distinct MHL indicate that both martensite and austenite phases can coexist in the region of irreversibility. On the heating envelope curve MHL starts to develop from A_s = 209 K, while on the cooling envelope MHL exist below M_s = 225 K, which constitute the boundaries for the region of phase coexistence. The observed thermal hysteresis and minor hysteresis loops support first order nature of the transition along with the phase coexistence in the irreversible region.

(Contributed by: S. Majumdar; subham@cat.ernet.in and V. K. Sharma)

A.6 Optical design of XRF microprobe beam line on Indus-2

Microprobe X-ray fluorescence (μ-XRF) and X-ray fluorescence (XRF) are powerful tools for determination of elemental heterogeneity and elemental composition of materials. With synchrotron radiation as the source, the sensitivity of these techniques can improve considerably. It is proposed to install a XRF microprobe beam-line on Indus-2. The basic applications are micro mapping of elemental heterogeneity and trace element analysis. Optical design of the beam line is completed.[CAT 2005-10]. The optical layout is given in fig. A.6.1.

Obtaining small spot size with maximum flux at the sample position has been the principal design consideration in this beam line. Apart from this, controllable energy resolution and spot size are other two principal features of the beam line. The objectives have been achieved by using asymmetrically cut Si (111) double crystal monochromator as dispersive optics and Kirkpatrick Baez (KB) mirror pair as focusing optics. The ray tracing simulations of the described design yield spot size of approximately 2μm (H) × 9μm (V) (fig. A.6.2) with ~ 10^8 photons/sec and energy resolution (E/ΔE) ~1000 at 10 keV photon energy. The beam line will operate in 3-20 keV photon energy range. The lower energy limit is defined by transmission through Be window and air where as the upper energy limit is defined by the cut off energy of the Pt coating of the mirrors of KB mirror system.

The first crystal of the monochromator will have -5^0 asymmetric angle with (111) plane of silicon, and the second crystal will have 5^0 asymmetric angle. Because of greater incident rocking curve width of the first crystal, the monochromator will pass higher flux compared to symmetric cut crystal monochromator. A slit before the first crystal of the monochromator will control the energy resolution of the beam line. With a controlled slit opening, the beam line can provide (E/ΔE) ~ 10,000 which is suitable for X-ray absorption spectroscopy, and total reflection X-ray fluorescence class of experiments. When the slit is wide open to allow the whole vertical divergence, the beam line can provide ~ 10^{10} photons/sec on a spot of size 20mm(H)×5mm(V) in unfocused mode.

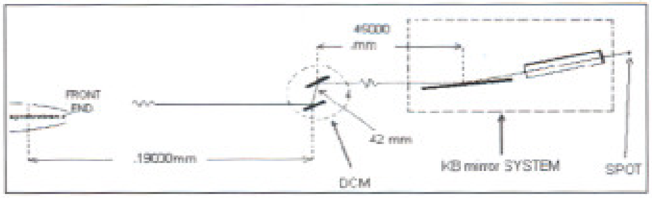

Fig. A.6.1 Optical design of the XRF microprobe beam line on Indus- 2

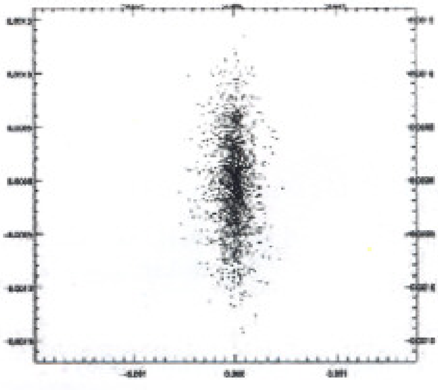

Fig. A.6.2 Spot on the sample

Two elliptical mirrors in KB arrangement focus the beam in vertical and horizontal direction. The mirrors are platinum coated and operate at grazing angle of 3.9 milliard. The horizontal and vertical acceptance of the beam line is defined by the acceptance of the 1st and 2nd mirror which is ~ 30 μrad. Both the mirrors can be removed to provide unfocused beam, which can be collimated to required size by high precision slits. The parameters of the second mirror can be changed to get a required spot size. Also the second mirror can be removed from the beam path to get vertically focused beam whose horizontal size can be controlled by high precision slits.

Ray tracing simulations are done with 10A° surface roughness on the mirror surface. The meridional slope error was 4.8 μrad and sagittal slope error was 8.9 μrad. The height of heat bump on the first crystal of the monochromator was taken into consideration at photon energy of 3 keV. The calculations were done by considering 300mA current in Indus-2 storage ring with 2.5GeV electron energy. The detail ray tracing and calculations were done by RAY and SHADOW simulation programs and XOP.

(Contributed by : Arijeet Das; arijeet@cat.ernet.in, A.K. Sinha and R.V. Nandedkar)

A.7 Data acquisition system (DAS) for reflectivity beam line on Indus-1

A DAS has been developed for reflectivity beamline on Indus-1. Its function pertain to control/monitor the following components of beam line:

1. Rotation of the toridal grating in the grazing incidence monochromator tracked by an encoder on serial bus.
2. Goniometer motions involving three-axes movements of three stepper motors, one for rotating the sample, second for rotating the detector and third for providing translation motion to the sample. Software controls the motion of these stepper motors using a driver card residing on PCI bus.
3. Synchrotron radiation photon beam current monitors on GPIB bus
4. Synchrotron radiation electron beam current monitor on a serial bus.
5. Continuous scan mode, which has increased the data acquisition rate significantly, which in turn saves significant beam time.

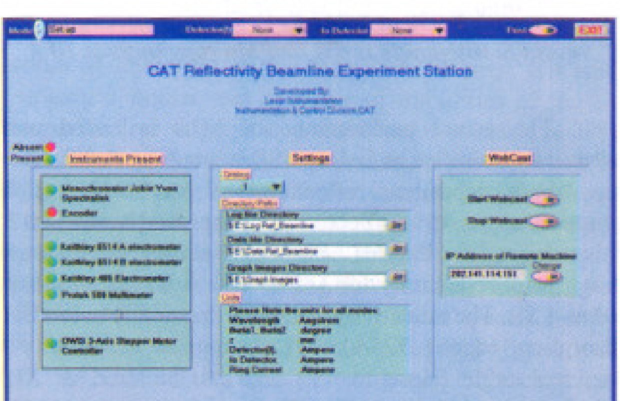

Fig. A.7.1 Main control panel for reflectivity beam line software

This LabView based software checks which of the instruments are connected and available. It further allows the user to select any of the following experiment modes:

i) Wavelength Scan	ii) Angle Scan
iii) Time Scan	iv) Continuous scan

The software acquires and on line plots of direct and reflected beam currents and ring current as a function of wavelength, angle or time depending on the mode. Various beamline, experiment and user defined parameters are stored in a log file. There is an option to store graph images for ready reference. File name is generated automatically based on experiment mode, date, time and user defined filename field. The experiment panel can be viewed on a remote PC anywhere on the network (fig. A.7.1). Earlier data can be overlaid on the graph for comparison purpose. Important parameters are saved in a configuration file for use in the successive runs.

(Contributed by : Shradha Palod; shradha@cat.ernet.in, P.P. Deshpande, V.P. Bhanage, M.H. Modi, A.G. Bhujle)

A.8 X-ray standing wave characterization of layered materials

Angle dependent grazing incidence X-ray fluorescence (GI-XRF), is another variant of total reflection X-ray fluorescence (TXRF) technique. By changing the incidence angle, the depth sensitivity of a layered material can be enlarged to nanometer regime. X-ray standing wave (XSW) effects occur in multilayer Bragg peak region as in perfect crystal.

Divergence of incident primary beam is one of the major sources of systematic error in X-ray standing wave characterization of single and multilayer thin films. Primary beam divergence significantly alters XSW profile of a layered material and can lead to large errors when used with higher excitation energies. These errors can be corrected by introducing beam divergence effects in the model calculations. In the present study we have evaluated optimum beam divergence below which the primary beam divergence effects need not be incorporated. For example, a primary beam of divergence 0.005° can be used with confidence in case of Mo-Kα excitation for XSW characterization of multilayers. On the other hand, this requirement of beam divergence can be relaxed up to 0.01° for Cu-Kα excitation.

Fig. A.8.1 shows the measured GI-XRF profile and reflectivity profile of a Fe/Si multilayer of parameters N = 10, d=16.8nm, Γ = 0.262 using Cu-Kα excitation energy. These ML samples were prepared using an ion beam sputtering system developed in-house. The measured GI-XRF profile